HYDROXYAPATITE INFLUENCE ON THE THERMAL AND MECHANICAL PROPERTIES OF A HIGHLY POROUS BONE CEMENT

Carlos J. Montaño[1*], Bruno R.S. Lemos[2], Maria I. Yoshida[2], Natanael G.S. Almeida[3], Tarcísio P.R. Campos[1]

1: Departamento de Engenharia Nuclear, Universidade Federal de Minas Gerais, Av. Antônio Carlos, 6627. CEP 31270-901, Belo Horizonte - MG, Brasil

2: Departamento de Química - ICEx, Universidade Federal de Minas Gerais, Av. Antônio Carlos, 6627. CEP 31270-901, Belo Horizonte - MG, Brasil

3: Departamento de Engenharia Metalúrgica de Materiais, Universidade Federal de Minas Gerais, Av. Antônio Carlos, 6627. CEP 31270-901, Belo Horizonte - MG, Brasil

** e-mail: carlmont@ucm.es*

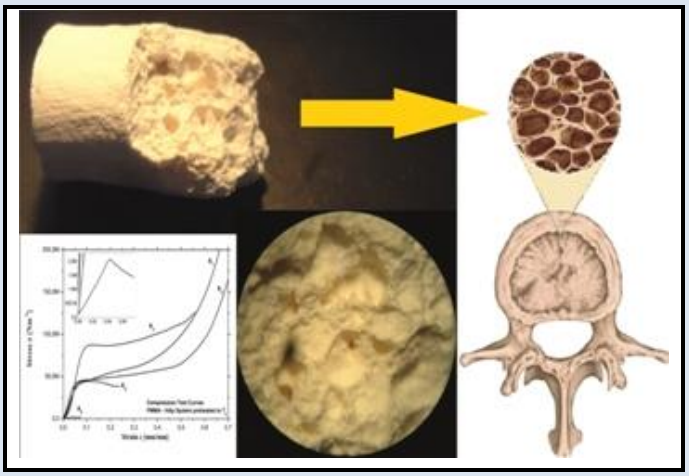

ABSTRACT

Background: Bone cements based on acrylics have been used in different orthopedic procedures. Currently, the PMMA+HAp system is used as bone cement in a minimally invasive procedure known as Vertebroplasty. In this paper, the main goal was to study the Hydroxyapatite influence on the thermal and mechanical properties of a non-commercial bone cement. The relationship of the glass transition Tg with its mechanical properties of the samples was also investigated. Materials and Methods: The bone cement as (1-x)PMMA-xHAp binary system was prepared in six distinct concentrations, such that [x] parameter is the concentration varying from 0.0 up to 0.5. The Hydroxyapatite (HAp) was synthesized using a sol-gel procedure following calcination by thermal treatment. The composite was prepared by mixing Polymethylmethacrylate (PMMA) and HAp. Differential scanning calorimetry (DSC), thermogravimetric analysis (TGA) and mechanical compressive strength (CS) were used to study the thermal and mechanical properties. The DSC and TGA thermal profiles as a function to concentration [x] were presented. Results: The concentration at x = 0.5 or x5 exhibited mechanical behavior similar to porous tissues compared with bone. The CS lies in a range of 1.71 - 7.37 MPa and the glass transition temperature Tg = 102.57 °C. Conclusions: There are direct relationships between the thermoplastic features of the PMMA+HAp system and its mechanical and thermal properties as a function of the biophosphonate concentrations ratio.

Keywords: *Bone Cement, DSC, Glass Transition, Compressive Strength.*

Recibido: 04-02-2020 ; **Revisado:** 02-09-2020

Aceptado: 09-09-2020 ; **Publicado:** 16-02-2021

DOI: 10.5281/zenodo.7397045

pISSN: 0255-6952 | eISSN: 2244-7113

Rev. LatinAm. Metal. Mat. 2021; **41** (1): 21-33

INFLUENCIA DE LA HIDROXIAPATITA EN LAS PROPIEDADES MECÁNICAS Y TÉRMICAS DE UN CEMENTO ÓSEO ALTAMENTE POROSO

RESUMEN

Antecedentes: Los cementos óseos basados en acrílicos han sido usados en diferentes procedimientos ortopédicos. Actualmente, el sistema PMMA+HAp es usado como cemento óseo en un procedimiento mínimamente invasivo conocido como Vertebroplastía. En este artículo, el objetivo principal fue estudiar la influencia de la Hidroxiapatita en las propiedades térmicas y mecánicas de un cemento óseo no comercial. La relación de la transición vítrea Tg con sus propiedades mecánicas también fueron investigadas. Materiales y Métodos: El cemento óseo como sistema binario (1-x)PMMA-xHAp fue preparado en seis concentraciones distintas, de modo que el parámetro [x] es la concentración que varía desde 0.0 hasta 0.5. La Hidroxiapatita (HAp) se sintetizó usando el procedimiento sol-gel después de la calcinación por tratamiento térmico. El compósito se preparó por la mezcla de Polimetilmetacrilato (PMMA) y HAp. La calorimetría de barrido diferencial (DSC), el análisis termogravimétrico (TGA) y la resistencia mecánica a la compresión (CS) fueron usadas para estudiar las propiedades térmicas y mecánicas. Los perfiles térmicos DSC y TGA como una función a la concentración [x] fueron presentados. Resultados: La concentración en x = 0.5 o x5 exhibió un comportamiento mecánico similar a los tejidos porosos comparados con el hueso. La CS se encuentra en un rango de 1.71 -7.37 MPa y la temperatura de transición vítrea Tg = 102.57 °C. Conclusiones: Hay una relación directa entre las características termoplásticas del sistema PMMA+HAp y sus propiedades térmicas y mecánicas como una función de la razón de concentraciones de biofosfanatos.

Palabras Claves: *Cemento óseo, DSC, Transición vítrea, Resistencia a la compresión.*

1. INTRODUCTION

The pathologic fractures have often occurred under normal physiologic stress in patients with spinal metastasis. The fracture occurs causing a partial or total damage of the vertebral body [1]. In the oncology cases, bone metastasis can significantly affect a patient's quality of life due to disabling pain, fractures or even paralysis by spinal cord compression [2]. Radiovertebroplasty has been early suggested to be similar to Vertebroplasty; however, with the insertion in situ of a radioactive cement [3]. Already, this has been studied by means of a computational simulation in which the dose delivered from the mixture between bone cement based on PMMA acrylics and radioisotope of interest as Sm-153 or Ho-166 targeting Hydroxyapatite (HAp) was spatial addressed in a computational vertebral phantom [4, 5]. The absorbed dose was also evaluated by MCNP-5 Monte Carlo Computer Code with P-32, Ho-166, Y-90, F-18, I- 125 and Tc-99m isotopes homogeneously distributed on the vertebrae. Both studies have been shown the spreading of the absorbed spatial dose being very limited into beta emitters range due to improvement in metastatic lesions [5-7]. HAp Nuclear features doped with Sm-152 and Ho-165, their decay processes, radionuclide contaminants and the activation process in a research reactor have been addressed, demonstrated the viability of producing radioactive cement in a neutrons low-flux reactor-type. Although the nuclear proprieties on the HAp-153Sm and HAp-166Ho bioceramics coupled with radioactive sources were presented by Donanzam et al. [4]; thermal and mechanical properties from based on PMMA+HAp system still no researched fully.

Thermal, morphological and mechanical properties on the PMMA electrospun nanofibers were studied. DSC was carried out to determine the phase change by increasing the PMMA/NaCl solution concentration. The results showed that the Tm (melting temperature) for a first glass transition was almost 116.19 °C to 2 samples with 12.5 and 15 % weight for the concentrations i.e. invariant with NaCl concentration. Nonetheless, the second glass transition temperatures were 121.58 °C to 12.5 % weight and 123.06 °C to 15 % weight for a second thermal anomalous, confirming that the crystallinity of the fibers of PMMA/NaCl increases with concentration [8, 9]. On the other hand, higher value of the glass transition temperature Tg yields stable thermally fibers [8, 10]. Also, this was reported an initial decomposition temperature of the PMMA powder at 140 °C and to PMMA/NaCl fibers at 302 and 320 °C respectively. This phenomenon is due to the sub-products during the thermal degradation process [8, 11]. Other studies on TG-DTA were developed in HAp to know the decomposition process attributed to nitrates and urea thus this being a largest weight loss. This is important to note that synthesis' methods based on HAp in both works are different. On the other hand, there are many positive aspects achieved when heat treatment at 800 °C was included [12]. Another author presents an exothermic peak due to the combustion of organic components around 300 °C to results with TG-DTA. The crystallinity increased when the heat treatment is close to 700 °C [13].

Also a mechanical properties study was applied only to behavior analysis about ultimate tensile strength (UTS) from nanofibers made with PMMA/NaCl ratio, which developed in the range 1 – 3 MPa. The modulus of the parallel layers in the nanofibers was studied with a value of 52.3 ± 5.2 MPa. A mechanical result important occurred where the layers arranged in cross its modulus was 26.1 ± 4.0 MPa [8, 14]. Based on previous work, Akhtar et al. in 2015 conclude that the nanofibers PMMA/NaCl, with optimal mechanical behavior, these can be used for applications in cell growth that are deposited on these PMMA nanofibers looms for biomedical and pharmaceutical areas [8]. Others studies on morphological and mechanics based on bone cement samples present compression properties than achieve values 71 and 95,5 MPa with an high pores amount and diameter higher to 66 µm [15, 16].

There are review studies about basic concepts on biomechanics and some bone properties [17], in which the biomechanical characteristics of the porous tissues could be appreciated [18]. In these reviews, the stress vs strain profiles in an elastic and plastic region can be classified. In these studies were obtained strength values for cortical bone from 167 - 213 MPa and Young's modulus between 14.7 - 34.3 GPa. For spongy bone, the strength varies from 1.5 - 9.3 MPa and the Young's modulus between 10 – 1058 MPa were presented by Caeiro et al. [18]. Such data can be addressed to qualify synthetic biomaterials as bone substitute in comparison to natural bone. These acrylic-based

biomaterials combined with HAp particles improve biocompatibility with tissues by increasing osteoconduction of the bone implant [19, 20]. The increase in porosity in these bone implants known as spacers in the orthopedic field provide an optimal environment for protein adhesion and osteoblast proliferation which expresses greater biomaterial functionality for various applications [21-23].

Our proposal research has as main goal to study the thermal and mechanical properties from a bone cement based on PMMA+HAp system with higher HAp concentration non-commercial type. The interest in the PMMA+HAp system is due to improvement its porosity when HAp compound is increased in the macroaggregate system. Such system can be applied in cold condition (non-radioactive) as bone implants, as bond cements for restoration of fractured parts, or in hot condition (radioactive) as a matrix of supporting radionuclides in treatments of bone metastases PMMA+HAp-^{153}Sm and PMMA+HAp-^{166}Ho.

2. MATERIALS AND METHODS

2.1. HAp Synthesis.

The HAp was synthesized by the sol-gel method according to Donanzam *et al.*, Campos *et al.* and Legeros *et al.* [3, 4, 24, 25]. The reagents used for the HAp synthesis were 3.937 g of calcium nitrate ($Ca(NO_3)_2{\cdot}4H_2O$), 0.69 mL of phosphoric acid (H_3PO_4), 1 up to 2 mL of methanol CH_3OH as a catalyst for starting reaction and deionized water as solvent in excess. After mixing the components, the solution was rested for 24 h in a closed beaker. Precipitation, nucleation and formation of colloids had occurred. Subsequently the sample was heated in an oven. The temperature started at room temperature ramped to 80 °C at a rate of 0.306 °C·min^{-1}, holding 360 min at the 80 °C isotherm, subsequently ramped to 100 °C at the rate of 0.333 °C·min^{-1} holding 720 min at 100 °C isotherm. At the calcinations, the sample was heated from room temperature to 720 °C at a rate of 6 °C·min^{-1}, following by a 60 min at 720 °C isotherm. After cooling, the HAp samples were macerated to powder.

2.2. PMMA-HAp composite preparation

HAp powder was mixed in different proportions to PMMA in its powder presentation. The composite was prepared in cold based (non-radioactive) mixing PMMA ($[CH_2C(CH_3)(CO_2CH_3)]_n$), Hap $[Ca_5(PO_4)_3(OH)]$. Both PMMA and the instruments were cooled previously. The mixture was stirring. PMMA-HAp system was prepared with PMMA's micro-spheres copolymer mixed to the monomer Methyl Ethyl Methacrylate (MMA). The samples were prepared in accordance with the following concentrations [x_n, with n = 1, 2, 3, 4, 5, 6], such that x_1 = 0.00000, x_2 = 0.02167, x_3 = 0.09062, x_4 = 0.16619, x_5= 0.50000 and x_6 = 1.00000. The x_n is a value corresponding to x in the following system (1-x)$[CH_2C(CH_3)(CO_2CH_3)]_n$-x$[Ca_5(PO_4)_3(OH)]$ or (1-x)PMMA-xHAp.

2.3. Calorimetry DSC and Thermogravimetric TGA assays

The thermal analysis was performed by using the differential scanning calorimetry DSC-60 Shimadzu; measured in two-time intervals. The measurements were carried out in a dynamic N_2 atmosphere (50 ml/min) at a heating rate of 10 °C·min^{-1} with 45 °C – 210 °C temperature interval of interest and a mass of 1.52 up to 3.39 mg for DSC thermal analysis. The samples placed on the aluminum pan were kept in laboratory temperature and atmospheric pressure conditions. A second heating was performed at 30 °C up to 450 °C following the same heating rate. The thermogravimetric analysis (TGA) was performed using METTLER TGA/DSC 1 equipment. The heating rate was the same as in the DSC previously described and in a temperature range of 30 °C to 750 °C, using amount of 3,5 - 7 mg of samples in alumina crucible. With the help of the thermal history and the loss of mass of the samples, the analysis was carried out to calculate the transition temperature T_g (I) and the enthalpy of glass formation ΔH_f (I) in the bone cement samples for each concentration on the (1-x)PMMA-xHAp system.

2.4. Mechanical Assay

The same material was prepared for the mechanical analysis, except to the concentration x_6 since this could not keep in a compact volume. The design model for fracture was a cylindrical block of 20 mm height and 10 mm diameter approximately. An amount of 5 g of the composite (1-x)PMMA-xHAp was mixed with 1.5 mL of MMA monomer and cast. The catalyst component was introduced to start polymerization. The pieces were fractured a week after preparation. The trials were done in INSTRON

5582 equipment Series Dual Column Floor Frames. The data acquisition was performed by Bluehill© Software. The loading speed was automatically adjustable for each sample. The specimens were isothermally heated at the glass transition temperature T_g (I), found in the DSC analyses, for 30 min in duplicate. Subsequently, the mechanical compression was performed. The compressive strength was calculated from the load curve and the geometrical factor of each sample that is obtained from the cylindrical dimensions (see Tables 1 and 2). The values presented correspond to the statistical mean of three measurements.

Table 1. Mean values over geometrical dimensions of test blocks of the (1-x)PMMA-xHAp system without preheating

x_n	Block 1 [mm] ±0,01			Block 2 [mm] ±0,01		
	D_1	D_2	H	D_1	D_2	H
x_1	10,91	10,64	20,80	10,70	10,50	20,60
x_2	11,16	11,00	21,40	11,08	11,00	21,42
x_3	11,16	11,22	21,60	11,32	11,22	21,10
x_4	11,00	11,20	21,15	11,01	11,00	21,22
x_5	13,20	13,30	22,00	13,37	13,40	21,37

* D1, D2: diameters and H height, cylinders dimensions

Table 2. Mean values of the (1-x)PMMA-xHAp system with preheating at Tg, for distinct geometrical dimensions of the sample's blocks.

x_n	Block 1 [mm] ±0,01			Block 2 [mm] ±0,01		
	D_1	D_2	H	D_1	D_2	H
x_1	10,80	10,60	21,00	10,70	10,60	21,00
x_2	11,28	11,36	21,20	11,25	10,96	20,50
x_3	11,40	11,25	20,25	11,40	11,43	20,50
x_4	10,70	11,00	22,11	11,25	11,00	22,00
x_5	12,20	12,00	21,40	12,60	12,00	22,00

* D_1, D_2: diameters and H height, cylinders dimensions

The ratio *H~2D* was defined to reduce the effects of friction between the anvils and the specimen and avoid bending during compression. The Figure 1 displays the specimen model before and after the tests considering an ideal model with non-friction.

Equation 1 is presented in order to take into account the analytical development and thus the ideal geometrical condition of the samples is satisfied. Equation 2 allows to understand the axial compressive strength under the methodological conditions addressed.

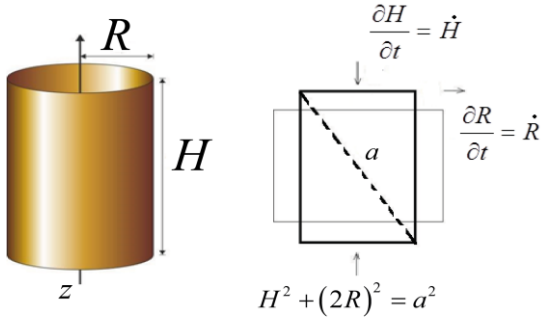

R = Radius, H = Height, D = Diameter = 2R

Figure 1. Diagram regarding the ideal dimensions of the test blocks, depicting the experimental conditions necessary for compression tests.

Considering that the material is isotropic, $\dot{H} = -\dot{R}$ having $a =$ constant, is satisfied during all compression tests. Equation 2 was used to achieve the stress-strain curves from the experimental force-displacement data. where σ being the axial compressive strength, as follows:

$$H^2 + (2R)^2 = a^2 \rightarrow 2H \cdot \dot{H} = -8R \cdot \dot{R} \qquad (1)$$

$$H \cdot \dot{H} = 2(2R)\dot{R} \rightarrow H = 2D \quad \text{Q.E.D.}$$

$$\sigma = \frac{F}{\pi D^2} \qquad (2)$$

3. RESULTS AND DISCUSSION

3.1. TGA profiles

TGA thermal profiles for the PMMA (copolymer)-HAp and PMMA+HAp systems were shown in Figure 2 and Figure 3. The mass in a range between 3,5 - 7 mg was used by TGA equipment. The TGA thermography results showed a significant mass loss after 100 °C for the x_i (i=1-6) concentrations that is associated with the water loss and degradation products. The Fig 2(a) shows greater mass loss in the concentration x_1, which contains a greater concentration of the polymer that corresponds to 100%. Above 250 °C, the boiling process of the substance begins, degrading mainly into CO_2 and

water steam. The loss of H_2O in the samples is due to the water retention in the bioceramics to a lesser degree and to the coupling of hydroxyl $(OH)^-$ that reacts with free hydroniums in form of water steam for samples with a HAp concentration [x]. The retention of water in HAp has been reported due to its hygroscopic nature and basically occurs due to the formation of dipole moments between phosphate groups and intermolecular hydroxyl $(OH)^-$ in the amorphous lattice of the bioceramic [26]. PMMA has been reported as a highly hydrophobic substance in its polymerizing form.

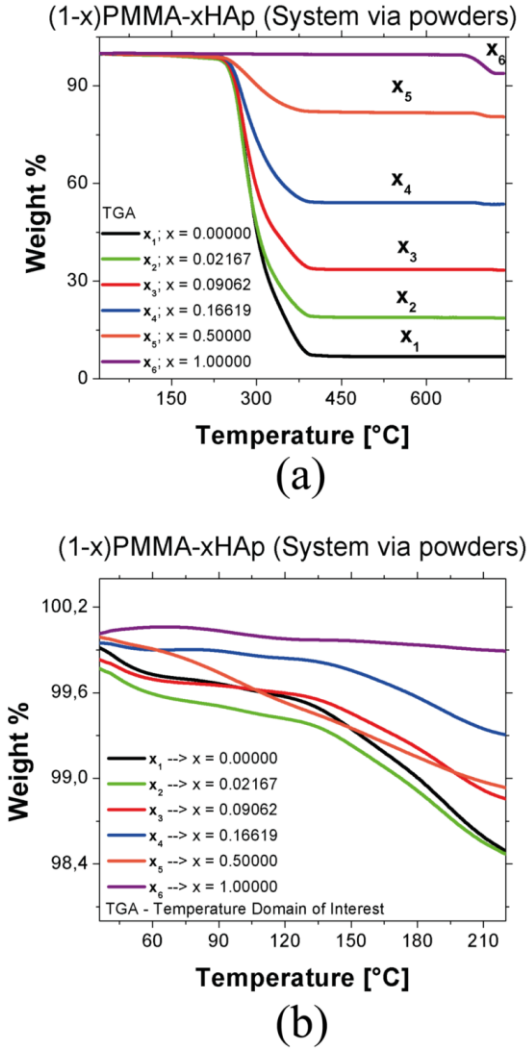

Figure 2. TGA heating profiles for x_i (i=1-6) concentrations of the (1-x)PMMA-xHAp system via powders to determine system's mass loss (a) among 35 – 751 °C (b) in TOI among 45 – 210 °C approximately.

Therefore, degradation and releasing CO_2 are dominant processes in the polymer [27]. Carbon residues constitute about 6% at sample x_1 when heating cycle finish to 751 °C. A higher HAp concentration into the samples produces a greater amount of residues associated with the bioceramics that reach the calcination temperature above 750 °C. The x_6 concentration consisting of the pure bioceramic shows a transition above 650 °C. Fig 2(b), there is mass loss with less than 1 % according to temperature domain of interest (TOI). A possible explanation may be due to a poor water's retention and the redistribution of the degradation segments that are coupled to both the polymer and the bioceramics through diffusion and self-diffusion processes.

In Fig 3(a), the polymerizing samples referring to the concentrations x_1 - x_4 show greater mass loss, even a little more than the samples of the system via powders. By-products and excess remnants of the polymerization reaction are degraded and released in the heating cycle, this being a cause for the greater loss of mass with respect to the system via powders. The graph also shows a very remarkable transition above 160 °C for the first four concentrations. In Fig 3(b) the maximum mass losses at 4 up 7 % were occurring after T_g glass transition. Also, significant mass losses were observed in Figs 2(b) and 3(b) at 110 to 160 °C intervals into TOI, above this temperature polymer melts.

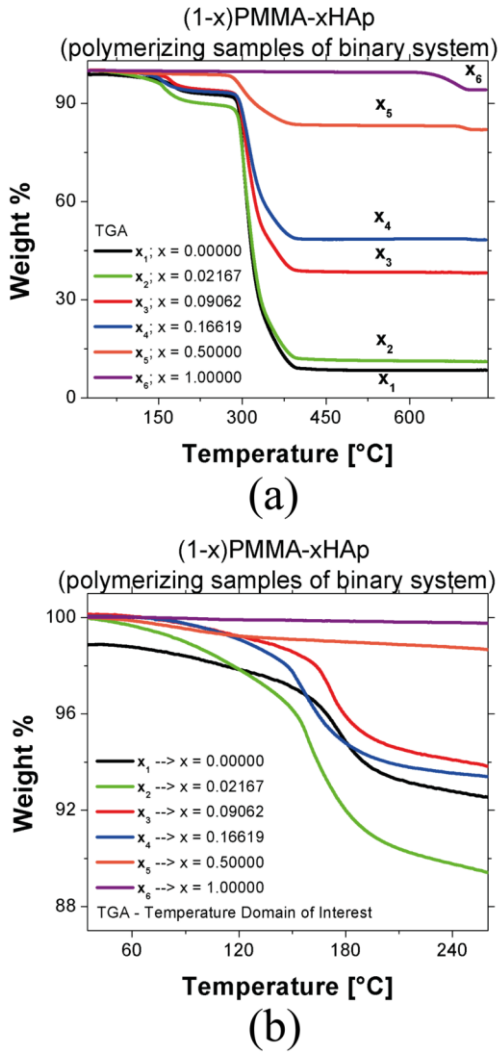

Figure 3. TGA heating profiles for x_i (i=1-6) concentrations of the (1-x)PMMA-xHAp polymerizing samples to determine system's mass loss (a) among 35 – 751 °C (b) in TOI among 45 – 240 °C approximately.

3.2. DSC profiles

The DSC thermal profiles for the PMMA(copolymer)+HAp and a PMMA+HAp system were shown in Figure 4 and Figure 5. A thermal anomaly has been confirmed after the second heating for the erasure in the thermal history and polymer stabilization for the analysis. The anomaly in DSC profiles were found in a temperature domain between 95 to 106 °C at the first four concentrations (x_1, x_2, x_3 and x_4). Comparatively, to the naked eye, the DSC thermograms on the second thermal scan show a constant negative slope from the x_1 - x_5 concentration, which indicates contamination of the samples due to the coupling of degradation by-products discussed above by the diffusion phenomenon. This negative slope of the thermal flux becomes less noticeable for bioceramics or concentrations with a higher proportion of HAp.

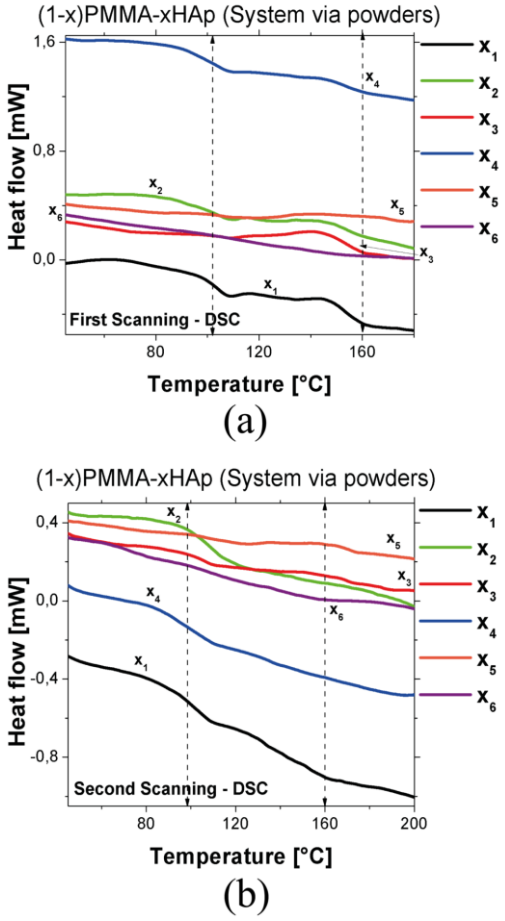

Figure 4. DSC heating curves for the six [x] concentrations of the (1-x)PMMA-xHAp system via powders in TOI between 45 – 200 °C. The Heat Flux is presented in [mW].

In the Figure 4 showed a thermal anomaly for the first four concentrations which held a higher PMMA ratio for each sample. The dotted line can guide the reader on the interest location in event described. The phenomena occurred in the samples with heat treatment which the baseline was corrected for each of the concentrations. The calculation T_g was made using the slope method with the help of DSC-60 Shimadzu analyzer. A relevant feature in the 96 to 106 °C domain is a possible T_g (I) glass transition reported previously [13,14]. The PMMA(Copolymer)+HAp system in powders showed a glass transition at T_g close to 102,57 °C in average. Here the crystallization phenomena were understood as the ratio between PMMA/HAp for

modulating to incorporate HAp microparticles between polymers chains. Indeed, the biophosphated calcium matrix should increment the crystallization level on the bone cement. Another important aspect was slightly more difficult to identify others glass transition temperatures reported by others authors. Probably due to different overlapping processes above glass transition mentioned already, this was no-possible to confirm. Despite this, it is possible to observe between 156 and 210 ° C for the powder system a possible transition prior to the polymer melting. In Fig 4(a) before T_g (II), at concentrations x_1, x_2, x_3 and x_4, a possible crosslinking associated with degradation products is observed, forming covalent bonds with the polymer chains. Despite this, in Fig 4(b) on the second heating, it can be observed that the T_g (I) remained relatively stable between 96 – 106 °C.

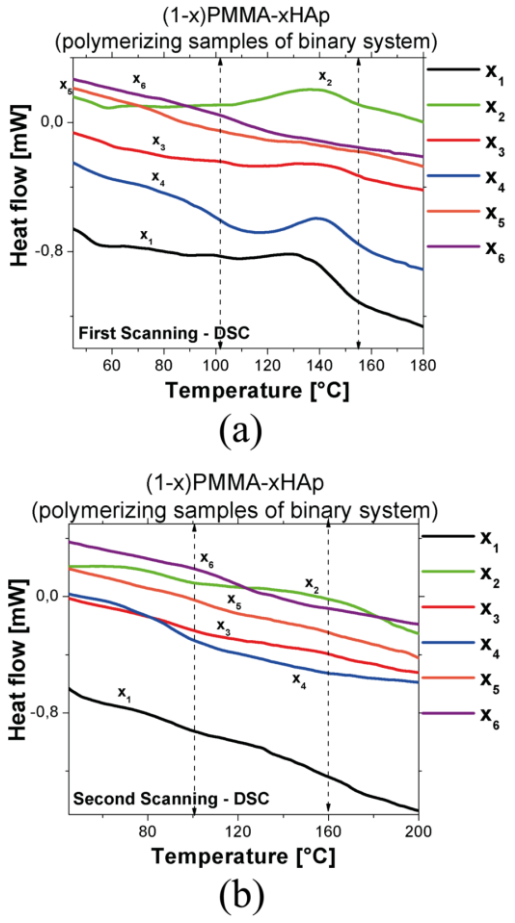

Figure 5. DSC heating curves for the six [x] concentrations of the (1-x)PMMA-xHAp polymerizing sample system in TOI between 45 – 200 °C. The Heat Flux is presented in [mW].

In Fig 5, the non-pure sample is most evident during the thermogram cycle in both the first and second scanning. In Fig 5 (a) the no pure sample is due to the remains of the polymerizing reagents as discussed in the TGA analysis. In addition, crosslinking is prominent at x_1 - x_4 concentrations due to the multiple formation of activated bonds by side reactions with remnants. An analysis is presented in the Tables 3 and 4 summarizing the calculation of T_g (I) and T_g (II) (glass transition phase I and II) and formation enthalpy ΔH_f of the glass phase for each of the concentrations of two types of samples.

The analyzer software uses the TGA and DSC results to determine the enthalpy of formation of the glass phase at the midpoint of the slope and the area under the curve [28, 29]. This analysis can be obtained by calculating the area under the curve on the specific heat plot of the sample at the critical temperature found in the TGA and confirmed by the DSC.

In Table 3 the T_g (I) do not follow a pattern and are relatively stable in each of the samples analyzed. The formation enthalpy of the glass phase (I) has a tendency to decrease as a function of the concentration of the polymer in the sample.

Table 3. Thermal analysis summary for the calculation T_g and ΔH_f of the (1-x)PMMA-xHAp system via powders

	(1-x)PMMA-xHAp Copolymer System				
x_n	Mass [mg]	T_g (I) [°C]	ΔH_f (I) [J/g]	T_g (II) [°C]	ΔH_f (II) [J/g]
x_1	2,58	**101,68**	25,82	156,60	22,18
x_2	1,52	**105,84**	24,73	212,52	11,70
x_3	1,94	**103,52**	4,87	169,86	1,61
x_4	2,09	**95,89**	8,24	175,03	3,72
x_5	1,57	**105,90**	6,77	169,81	4,86
x_6	1,72	- - - - -	- - - - -	- - - - -	- - - - -

* T_g (I), T_g (II): glass transition temperature (I) and (II)
** ΔH_f (I), ΔH_f (II): formation enthalpy

The x_3 concentration requires less energy for the glass phase formation, and this is precisely because in the first scanning a possible crosslinking is observed, which in the second scanning has defined a more intricate structure with less polymer in its natural state. The T_g (II) is highly oscillating and not

very stable, probably due to overlapping chemical interactions, although ΔH_f (II) has a tendency to decrease with the absence of the polymer.

The Table 4 shows a lower mean value T_g (I) than for the samples via powders. Furthermore, ΔH_f (I) exhibits a decreasing behavior when the concentration of the polymer is lower. The behavior of the glass transition (II) is similar to the samples via powders.

Table 4. Thermal analysis summary for the calculation T_g and ΔH_f of the (1-x)PMMA-xHAp polymerizing samples

	(1-x)PMMA-xHAp System				
x_n	Mass [mg]	T_g (I) [°C]	ΔH_f (I) [J/g]	T_g (II) [°C]	ΔH_f (II) [J/g]
x_1	1,93	**88,71**	44,67	171,42	37,95
x_2	1,92	**83,52**	10,82	179,40	7,88
x_3	2,89	**93,93**	6,46	168,24	8,04
x_4	3,00	**92,32**	4,89	154,63	8,48
x_5	3,39	**104,70**	1,49	199,40	5,14
x_6	2,06	- - - - -	- - - - -	- - - - -	- - - - -

* T_g (I), T_g (II): glass transition temperature (I) and (II)
** ΔH_f (I), ΔH_f (II): formation enthalpy

3.3. Mechanical strength

Two assays were performed to know the mechanical behavior of the cement as a function of the HAp concentration. Moreover, in the other case, to know the dependence on the concentration simultaneously with the blocks thermally treated around to the glass transition temperature. Figures 6(a) and 6(b) depicted the strength profiles to compression on the composite as a function of theirs x, x_i (i=1-5) concentrations in the PMMA+HAp system. A geometric factor was considered for each block with concentration [x_n].

The Table 5 summarizes compressive strength (CS) respect to HAp concentration on the binary system also shows the glass transition T_g for each sample. Glass transition temperature and the mass losses were relatively stable for the concentrations [x] at 0.0 up 0.5. This thermodynamic characteristic for each concentration allows to evaluate the mechanical behavior among all samples in a standard way.

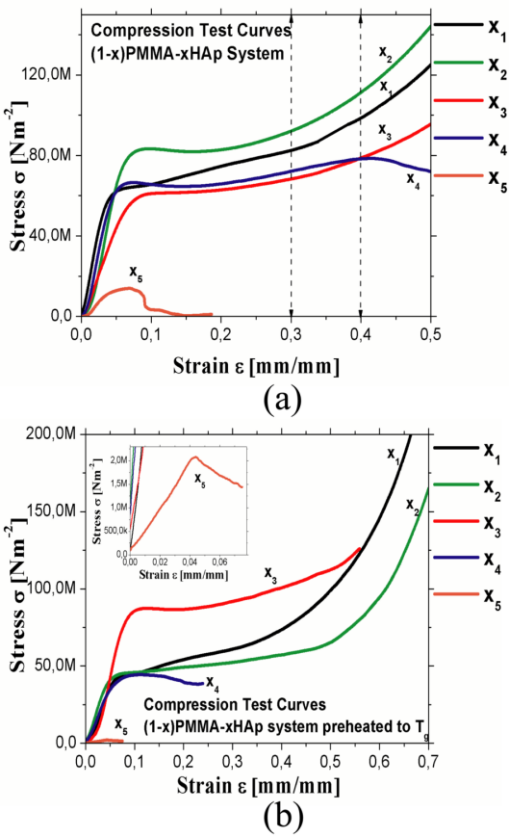

Figure 6. Compression profiles for the mechanical assay on the blocks with x_i (i=1-5) concentrations of the (1-x)PMMA-xHAp binary system, where (a) PMMA+HAp polymerized system without thermal treatment with a fracture domain at 0.30 – 0,42 % compression strain; and (b) PMMA+HAp polymerized system with thermal treatment of 30 min at T_g glass transition temperature.

Table 5. Thermo-mechanical properties of (1-x)PMMA-xHAp System.

x_n	[x]	T_g [°C]	TGA M. loss[%]	CS [MPa]	CS with T_g [MPa]
x_1	0.00000	101,68	4.02	64.44	84.00
x_2	0.02167	105,84	6.80	60.45	82.77
x_3	0.09062	103,52	4.33	87.60	70.13
x_4	0.16619	95,89	4.89	41.40	70.07
x_5	0.50000	105,90	< 1	19.50	**1.71–7.37**
x_6	1.00000	- - - - - -	< 1	- - - - -	- - - - - - -
*	Cortical or compact bone			167–213	- - - - - - -
**	Trabeculae or Spongy Bone			**1.5 – 9.3**	- - - - - - -

* and ** cited by Caeiro *et al.* [18]; CS—Compressive Strength;.

For high concentrations of the polymer, taking into account that the long ball-shaped carbon chains induce a high degree of intricacy, due to the covalent carbon bond formation. When the strain ratio exceeds the elastic region in samples with high polymer content, there is an irreversible spatial redistribution (permanent strain) of these covalent bonds until the sample's breaking point is reached. In accordance with the foregoing, the necessary energy that is applied to reach the fracture point where these redistributions of bonds occur, mainly for cement samples with high polymer content, in such a way that the plastic region increases and therefore its toughness resilience are higher.

For high amorphous HAp bioceramic concentrations in the test blocks, all positions of the bioceramic lattice includes Calcium, phosphate and hydroxyl groups joined low-energy bond which made it less intricacy structurally respect to polymer. About x_5 concentration, both the toughness and resilience is low because the area under curve is smaller, according with the structural and chemical arguments presented above over this bone cement. The compressive strength was studied on two groups of test blocks. The group without pre-heating showed high compressive strength while the group with pre-heating to T_g had a tendency with less plasticity region thus low toughness.

3.4. Stereo surface images for PMMA+HAp system samples

The Figure 7 shows images of the PMMA block surface without thermal treatment (x_1) Fig 7(a) and of a block with the highest concentration of HAp (x_5) with thermal treatment to T_g temperature as is presented in Fig 7(b).

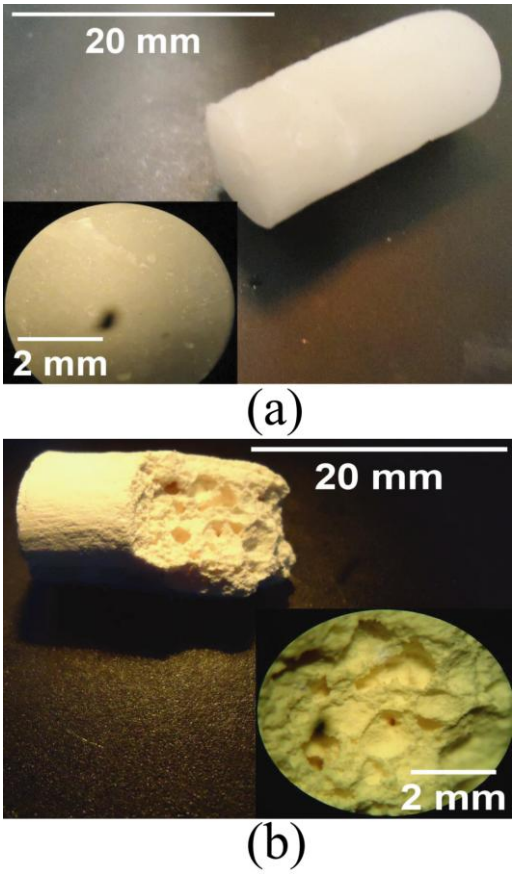

Figure 7. Stereoscopic images of the block surfaces, where (a) to PMMA only or x_1 concentration without thermal treatment; (b) to x_5 concentration parameter with thermal treatment for 30 min at the T_g glass transition temperature.

The binary PMMA+HAp system under study has been based on several commercial bone cements with a higher HAp's concentration in some samples. The PMMA polymerization is made with two products, a liquid presentation composed of dimers and other presentation in powder made by PMMA microparticles with a size between 30 to 80 micrometers. The polymerization process occurs by aggregation between monomers and PMMA microparticles to join each other forming amorphous sequential chain. At our PMMA+HAp composite preparation, the water solution modulated the heterogeneous phases of acrylic resulting in an increase in polymerization time (PT). The instrumentation and material cooling procedure also increased the PT due to the reduction on the intensity of the polymerizing effect that is proportional to the room temperature.

The pores' production *in situ* is very hard since these must follow a random pattern or anisotropic according to where the implant is located. The pores' production was understood as spontaneous defect in the material. The pores should be connected or have thin walls in which fluid can be diffused, allowing the plasma and bone marrow diffusions, in which angiogenesis and other vascularization processes should be performed facilitating all the natural biological phenomenon. This is very important to emphasize since all the thermal profiles were normalized with the maximum thermal power to evaluate how the present anomalies behave as a concentration's function on the bone cement. Another important aspect on the DSC analysis was to confirm the existence of a T_g glass transition in the temperature range that has already been mentioned by other researchers [13], which shall bring the question how the mechanical properties in the compound are varying when it has been treated thermally.

TGA analysis Fig 3 suggests the possibility to increase the polymorphic characteristics of the binary system with respect to promoting more defects associated with its porosity. Some reactions with gas-releasing start after the glass transition where the polymer chains interact with $(OH)^-$, producing water vapor and CO_2. These low mass losses depicted in Fig 2(b) confirm that calcium biophosphonates are only in the heterogeneous phase in the system which reduces the gas-releasing process due to the interaction with $(OH)^-$ groups and the polymer. The polymerized mixture in Fig 3(b) remains a much more intricate heterogeneous composite between calcium biophosphonates and polymer chains.

Considering the mechanical strength depicted in Fig 6(a), the region between the dotted lines shows a tentative to define the strain domain where the fracture on the material occurred. In principle, the modulus of compressive strength decreases with increasing HAp's concentration. In the Fig 6(b) observe that the plastic region is smaller for the concentrations x_4 and x_5, whereby it becomes clear that the material is more fragile. This is important to recall because the blocks were heated to the glass transition temperature in order to respond the question about how is the mechanical feature for the material after glass-transition temperature treatment. The Compressive Strength (CS) for the block of x_1 concentration parameter was one-third of the CS mean values to human cortical bone; while it was 15-fold for x_1 and 4-fold for x_5 higher to mean value to the human spongy bone. For the blocks with thermal treatment, the CS presents close to 30 % higher that without thermal treatment; although, for the concentration x_5 the CS values is in the range of the spongy bone tissue. Fig 7 shows the blocks surface morphology such that in Fig 7(a) corresponding to x_1 concentration sample presents no pore and Fig 7(b) is block corresponding to x_5 concentration sample shows pore production *in-situ* with large size.

4. CONCLUSIONS

In this study, it was possible to establish a direct relationship between the thermoplastic properties of the PMMA+HAp acrylic system and its mechanical properties so that changes as a function of the biophosphate concentration. The HAp concentration of the compound can be used to optimize its mechanical qualities for the purpose of a desired biomedical application. The biomechanical results for the concentration x_5 presented Compressive Strength values between 1.71 – 7.37 MPa such that there are similarity to porous bone studied by Caeiro *et. al* with values between 1.5 – 9.3 MPa according to Table 5 [18]. The greatest innovation reached in this work was to improve bone cement syntheses through the biochemical properties use to increase the porosity of the material reaching a range such that the bone marrow diffusion could occur more easily. An increase in the HAp amorphous polycrystalline structure favors the segregation interactions in different segments of the PMMA polymer due to its hydrophobic nature similar to the reactions among amphiphilic molecules and water. The pores' size is perceptible to the human eye very close to those found in the trabecular bone tissue itself. This phenomenon was optimized with the thermal treatment carried out on the samples at the glass transition temperature close to 102.57 °C. On the other hand, the possible dehydration reactions occurred in the material improving the formation of more pores and with larger size due to the release of water and CO_2 in the heterogeneous mixture.

5. ACKNOWLEDGEMENTS

The authors are grateful for the financial support from the CAPES, REBRAT-SUS project supported by CNPq. The corresponding author thanks to the PAEC OEA-GCUB 2014 program for the opportunity offered with the doctoral scholarship in this academic and research experience. Finally, the authors are grateful with Dra. Sonia Seger Pereira Mercedes (Dep. Engenharia Nuclear - Universidade Federal de Minas Gerais) for her valuable collaboration.

6. REFERENCES

[1]. Georgy BA. Am. J. of Neuroradiology. 2008;29: 1605-11.

[2]. Harel R, Angelov L. European J. Cancer. 2010; 46(15): 2696-707.

[3]. Campos TPR, Macedo RDA. Compósito Ósseo Radioativo. Instituto Nacional da Propriedade Industrial - INPI, editor. Brasil, 2006.

[4]. Donanzam B, Campos T, Dalmázio I, Valente E. J. Mater. Sci.: Mater. Med. 2013; 24: 2873-80.

[5]. Montaño CJ, Campos TPR. Acta Ortop. Bras. 2019;27(1): 64-68.

[6]. Hirsch AE, Medich DC, Rosenstein BS, Martel CB, Hirsch JA. Radiotherapy and Oncology. 2008;87(1): 119-26.

[7]. Hirsch AE, Rosenstein BS, Medich DC, Martel CB, Hirsch JA. Pain Physician. 2009;12:887-891.

[8]. Akhtar MN, Sulong AB, Karim SA, Azhari CH, Raza M. Iranian Poly. J. 2015;24: 1025-38.

[9]. Ji L, Medford AJ, Zhang X. Polymer. 2009;50:605-12.

[10]. Matabola K, De Vries A, Luyt A, Kumar R. Poly. Lett. 2011; 5 (7): 635-642.

[11]. Kaniappan K, Latha S. Int. J. ChemTech Res. 2011;3(2):708-715.

[12]. Bezzi G, Celotti G, Landi E, La Torretta T, Sopyan I, Tampieri A. Mat. Chem. Phys. 2003;78(3): 816-824.

[13]. Hwang K, Song J, Kang B, Park Y. Surf. Coat. Tech. 2000;123(2-3): 252-255.

[14]. Matthews JA, Wnek GE, Simpson DG, Bowlin GL. Biomacromolecules. 2002;3 (2):232-238.

[15]. Puska M, Moritz N, Aho AJ, Vallittu PK. J. Mech. Behav. Biomed. Mat. 2016;59:11-20.

[16]. Guadarrama Bello D, López Hernández M, Brizuela Guerra N. Rev. LatinAm Metal. Mat. 2011;31:91-98.

[17]. Guede D, González P, Caeiro J. Rev. Osteop. Metab. Min. 2013;5(1):43-50.

[18]. Caeiro J, González P, Guede D. Rev. Osteop. Metab. Min. 2013;5(2): 99-108.

[19]. Coughlin TR, Romero-Moreno R, Mason DE, Nystrom L, Boerckel JD, Niebur G, Littlepage LE. Curr. Drug Targ. 2017;18 (11):1281-1295.

[20]. Deng M, G Kumbar S, W-H Lo K, D Ulery B, T Laurencin C. Rec. Pat. Biom. Eng. 2011;4 (3):168-84.

[21]. Murugan R, Ramakrishna S. Biomaterials. 2004;25(17): 3829-3835.

[22]. Kim SS, Park MS, Jeon O, Choi CY, Kim BS. Biomaterials. 2006;27(8):1399-1409.

[23]. Ferraz MP, Monteiro FJ, Manuel CM. J. App. Biomat. Biomech. 2004;2: 74-80.

[24]. LeGeros R, Lin S, Rohanizadeh R, Mijares D, LeGeros J. J. Mat. Sci.: Mat. Med. 2003;14:201-209.

[25]. Chen J, Wang Y, Chen X, Ren L, Lai C, He W, Zhang QQ. Mat. Lett. 2011;65 (12):1923-1926.

[26]. Klimavicius V, Kareiva A, Balevicius V. J. Phys. Chem. C. 2014;118: 28914-28921.

[27]. Lozano K, Mina J, Zuluaga F, Valencia C, Valencia M. Dyna. 2013;80 (181):153-62.

[28]. Wunderlich B. Thermal analysis of polymeric materials: Springer Science & Business Media; 2005.

[29]. Montaño CJ, Checa O, Diosa JE, Vargas RA. Rev. LatinAm Metal. Mat. 2009; S1(2):509-513.

7. MINIBIOGRAFÍA DE AUTORES

CARLOS JULIO MONTAÑO VALENCIA, Physics - University of Valle (2009) - Colombia. Master in Biomedical Physics - Complutense University of Madrid (2014) - Spain. Ph. D. in Nuclear Sciences and Techniques, concentration area in Radiation Sciences from Federal University of Minas Gerais (2019) - Brazil. Currently, He acts as a Postdoctoral Resident in the Department of Nuclear Engineering – UFMG, with a project in progress belonging to PNPD / CAPES program in the area of Energy and Renewable Resources. (https://orcid.org/0000-0001-7125-9982)

BRUNO ROCHA SANTOS LEMOS. Bachelor in Chemistry (2007), M. Sc. in Chemistry (2010) and Ph. D. in Chemistry (2015) from the Federal University of Minas Gerais (UFMG). Since 2012, he has been a permanent professor at the Pontifical Catholic University of Minas Gerais (PUC-MINAS), working in the Department of Physics and Chemistry (DPCh) belonging to Institute of Exact Sciences and Informatics (IEScI). Since 2010, he has also worked as Postdoctoral Resident at UFMG, currently working in the thermal analysis laboratory of the Department of Chemistry (DCh) of the Exact Sciences Institute (ICEx). (https://orcid.org/0000-0001-7221-3492)

MARIA IRENE YOSHIDA. Bachelor in Chemical Engineering from Escola de Engenharia / UFMG (1976), M.Sc. in Chemistry from UFMG (1982) and Ph.D. in Chemistry from ICEx / UFMG (1993). She is currently Full Professor at the Federal University of Minas Gerais. Responsible for the Thermal Analysis Laboratory of the Department of Chemistry / UFMG. She works in Chemistry, with an emphasis on Trace Analysis and Environmental Chemistry and Thermal Stability of Solids working mainly on the following topics: thermal analysis, thermogravimetry, polymorphism and drug interactions. (https://orcid.org/0000-0002-6795-9457)

NATANAEL GERALDO E SILVA ALMEIDA. Bachelor in Mechanical Engineering from Pontifical Catholic University of Minas Gerais (2014), Master in Mechanical Engineering from Federal University of Minas Gerais (2017) and Ph.D. in Metallurgical and Mining Engineering from Federal University of Minas Gerais (2021). Has experience in Materials and Metallurgical Engineering, with emphasis on Mechanical Properties of Metals and Alloys, acting on the following subjects: mechanical forming, mechanical testing, characterization by scanning electron microscopy, EBSD and transmission electron microscopy. (http://lattes.cnpq.br/6100769047947778)

TARCÍSIO PASSOS RIBEIRO CAMPOS. Full Professor at the Federal University of Minas Gerais, responsible for the Ionizing Radiations Laboratory in the Department of Nuclear Engineering. Bachelor in Engineering from the Federal University of Minas Gerais (1983), Master in Nuclear Engineering from the Federal University of Rio de Janeiro (1985) in the area of Reactor Physics (Nuclear Resonances), Ph.D. in Nuclear Engineering - University of Illinois at Urbana Chamapaign - UIUC/USA (1993) and post- PhD at Massachusetts Institute of Technology - MIT/USA (1998) in the MIT-Harvard research program, as Fulbright Fellow. (https://orcid.org/0000-0003-1476-3474)